Journal of Power Sources 242 (2013) 503–509

Contents lists available at SciVerse ScienceDirect

Journal of Power Sources

journal homepage: www.elsevier.com/locate/jpowsour

Adsorption and oxidation of acetaldehyde on carbon supported Pt, PtSn and PtSn-based trimetallic catalysts by in situ Fourier transform infrared spectroscopy

Seden Beyhan [a,b,*], Jean-Michel Léger [b], Figen Kadırgan [a]

[a] Department of Chemistry, Faculty of Science and Letters, Istanbul Technical University, 34469 Maslak, İstanbul, Turkey
[b] Electrocatalysis Group, IC2MP, UMR 7285, CNRS, Université de Poitiers, 40 avenue du Recteur Pineau, 86022 Poitiers Cedex, France

HIGHLIGHTS

- Acetaldehyde adsorption and oxidation on Pt, PtSn, PtSn-based ternary catalysts.
- PtSn is not selective for CO_2 production with its weak CO band intensity.
- Adding Ni, Co, Pd and Rh to Pt–Sn favours the cleavage of C–C bond in acetaldehyde.

GRAPHICAL ABSTRACT

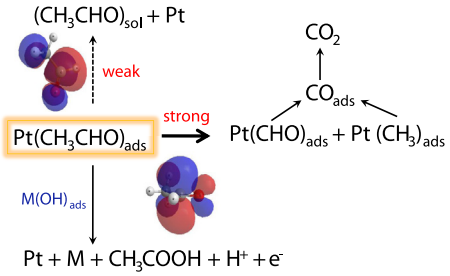

ARTICLE INFO

Article history:
Received 28 January 2013
Received in revised form
29 April 2013
Accepted 23 May 2013
Available online 5 June 2013

Keywords:
In situ infrared spectroscopy
Acetaldehyde oxidation
Platinum-tin catalyst
Trimetallic catalyst

ABSTRACT

The adsorption and oxidation of acetaldehyde on carbon supported Pt, $Pt_{90}Sn_{10}$ and $Pt_{80}Sn_{10}M_{10}$ (M = Ni, Co, Rh, Pd) catalysts have been investigated by using in situ Fourier transform infrared (FTIR) spectroscopy. The result revealed that $Pt_{90}Sn_{10}/C$ catalyst is not very efficient for the conversion of acetaldehyde to CO_2 due to the weak adsorption of acetaldehyde in the presence of Sn. However, the addition of a third metal to Pt–-Sn facilitates the C–C bond cleavage of acetaldehyde. It seems that acetaldehyde is adsorbed dissociatively on the surface of $Pt_{80}Sn_{10}Ni_{10}/C$, $Pt_{80}Sn_{10}Co_{10}/C$, $Pt_{80}Sn_{10}Rh_{10}/C$ catalysts, producing CH_3 and CHO adsorbate species, which can be further oxidized to CO_2. However, the pathway forming CO_2 for $Pt_{80}Sn_{10}Pd_{10}/C$ catalyst mainly originates from the oxidation of CH_3CO species. Thus, the presence of third metal in the PtSn catalyst has a strong impact upon the acetaldehyde adsorption behaviour and its reaction products.

1. Introduction

It is generally accepted that the main oxidation products during acetaldehyde oxidation are CO_2 and acetic acid. However, the product yield depends on the acetaldehyde concentration, temperature, electrode potential, and catalyst material. Rasch and Iwasita [1] have investigated the yields of products of acetaldehyde oxidation on polycrystalline Pt electrode in acidic solution using in situ Fourier transform infrared (FTIR) spectroscopy as a function of acetaldehyde concentration (0.1 and 1 M). It was shown that for concentrated acetaldehyde solutions (1 M) and high potentials, both acetic acid and CO_2 were detected to the close neighbourhood of the electrode surface. Nevertheless, only CO_2 was produced for low acetaldehyde concentration (0.01 M); and moreover, the quantity of produced CO_2 became similar at both low and higher acetaldehyde concentrations. The final product of CO_2 results from

* Corresponding author. Department of Chemistry, Faculty of Science and Letters, Istanbul Technical University, 34469 Maslak, Istanbul, Turkey. Tel.: +90 212 285 72 70; fax: +90 212 285 63 86.
E-mail addresses: beyhanse@itu.edu.tr, seden1980@yahoo.com (S. Beyhan).

0378-7753/$ – see front matter © 2013 Elsevier B.V. All rights reserved.
http://dx.doi.org/10.1016/j.jpowsour.2013.05.112

the oxidation of adsorbed CO, which seems to originate either from the oxidation of acetic acid or from the dissociative adsorption of the acetaldehyde. Pastor et al. [2,3] used differential electrochemical mass spectroscopy (DEMS) techniques to study the acetaldehyde reactions on Pt and Rh electrodes in acid solution. They identified that acetic acid and CO_2 were the electrooxidation products detected whereas methane and ethane were equally formed during the reduction of the adsorbed types. However, ethane was detected at only Pt electrode. Kokoh et al. [4] performed in situ FTIR spectroscopy and high performance liquid chromatography (HPLC) techniques for electrooxidation of acetaldehyde on Pt-based ruthenium and osmium alloy electrodes. They showed that for these two electrodes the presence of acetic acid in majority, formic acid and CO_2 in small amount, suggesting low-level poisoning by CO_{ads} due to the synergetic effect of Ru near the Pt sites.

Literature concerning to the electrooxidation of acetaldehyde refers mainly to Pt surface. Surprisingly there have been no in situ FTIR studies on reported for the reactivity of acetaldehyde on carbon supported PtSn and PtSn-based trimetallic catalyst materials. It is well known that the alloying Pt with Sn generally weakens the adsorption energy of small organic molecules such as ethanol, methanol and strongly inhibits dehydrogenation reactions. Therefore, it is an interesting question whether or not the presence of third metal in the PtSn/C catalyst will lead to an increase in the reactivity of acetaldehyde. Indeed, a deeper understanding of the reaction mechanism of acetaldehyde on Pt, PtSn and PtSn-based trimetallic surfaces will be very helpful in developing catalyst for the electrooxidation of ethanol since acetaldehyde is a key intermediate in the ethanol oxidation reaction [5–10]. This paper will focus on identifying the intermediates and products of acetaldehyde adsorption and oxidation on the carbon supported Pt, PtSn and PtSn-based trimetallic catalysts by using in situ FTIR spectroscopy and discussing the reactivity of acetaldehyde by the addition of Ni, Co, Rh and Pd to PtSn/C.

2. Experimental section

2.1. Preparation of electrodes

Carbon supported Pt, bimetallic $Pt_{90}Sn_{10}$ and trimetallic $Pt_{80}Sn_{10}Y_{10}$ (Y = Ni, Co, Rh, Pd) catalysts were prepared by the Bönnemann method [11], but slightly modified as described in our previous papers [12,13]. Catalyst ink was prepared by dispersing of 25 mg of catalyst powder in a 2.5 ml of water solution containing 0.5 ml 5% Nafion® via sonication for two hours. 8 μl of the resulting ink was pipetted onto a glassy carbon disk working electrode (disk of 7 mm diameter) by micro syringe and dried at room temperature, which was polished with 0.5 μm alumina before each deposition to obtain the mirror-finished surface in order to obtain good reflectivity. All the measurements were done at least three times with freshly prepared electrode at room temperature.

2.2. In situ FTIR measurements

FTIR spectra were collected by a Fourier transform infrared spectrometer (Bruker IFS 66v) with an incidence angle of 65°. This instrument is equipped with nitrogen-cooled HgCdTe detector. Parallel-polarised light was obtained from a BaF_2-supported Al grid polarizer. The cell potential was controlled using an LB 81 Wenking potentiostat and a Hi-tek waveform generator, connected to a BD 90 XY recorder. The spectral resolution was 4 cm^{-1}. Data acquisition and processing were performed using a computer with OPUS 5.5 software (developed by Bruker).

The IR light beam passes entirely a chamber under vacuum before the observation of reflectance spectra of the electrode–electrolyte interface through the IR window (CaF_2) of a conventional thin layer spectroelectrochemical cell. Electrolyte solution of acetaldehyde (Merck) was prepared with Millipore water (18 MΩ cm) by taking necessary volume from the stock solution which was previously stored in a freezer due to its low boiling point (21 °C), and 0.1 M $HClO_4$ (Merck, Suprapur) as a supporting electrolyte. Before spectrochemical measurements, the solution was purged with pure nitrogen (U quality from L'air Liquide). Au wire was used as the counter electrode, and a reversible hydrogen electrode (RHE) was used as the reference.

Using the single potential alteration infrared reflectance spectroscopy (SPAIRS) method, the electrode reflectivity RE_i are regularly recorded each 0.05 V during the first cyclic voltammogram (CV) scan rate at 1 mV s^{-1}. Each spectrum resulted from the co-addition of 128 interferograms. The data acquisition required 50 s, i.e. over 0.05 V steps from 0.05 to 1 V vs. RHE increased the potential. The results were displayed as $\Delta R/R = (RE_2 - RE_1)/RE_1 = -\Delta A$, where RE_1 is the reflectivity at potential E_1 and RE_2 the reflectivity at the potential E_2. For the calculation, E_1 can be taken at the initial potential of the CV; E_2 is some value along the CV. If $E_1 < E_2$, a positive absorption band means the consumption of species at the sample potential and a negative absorption band indicates the production of species at the electrode surface. The absorption bands are commonly observed as a bipolar shape when the adsorbed species is stable at the two potentials, due to the Stark effect [14,15]. The band is unipolar, if the adsorbed molecule is stable at one potential and oxidized or reduced at the second potential. In this work, in order to detect the formation and the evolution of the CO band, a series of SPAIR spectra was calculated using reference spectra at 0.9 V vs. RHE where CO totally oxidized [16]. To follow the appearance of CO_2, a reference spectrum was similarly recorded at 0.05 V vs. RHE, a potential at which CO_2 is absent from the solution.

3. Results and discussions

Fig. 1 shows the linear sweep voltammograms of the carbon supported Pt, PtSn and PtSn-based trimetallic catalysts synthesized by the Bönnemann method in 0.1 M $HClO_4$ + 0.1 M CH_3CHO

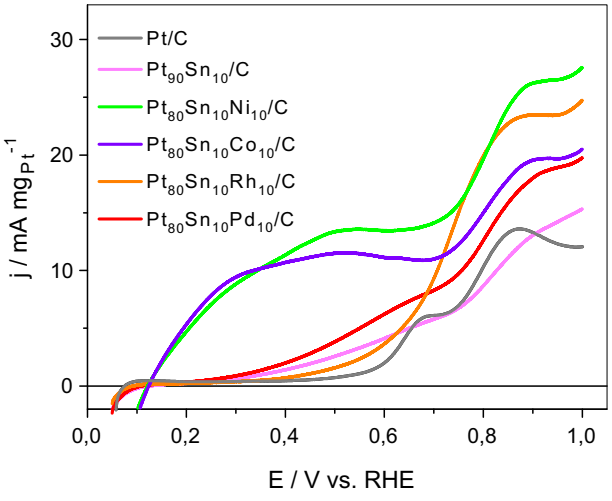

Fig. 1. Linear sweep voltammograms for the electrooxidation of 0.1 M CH_3CHO in 0.1 M $HClO_4$ solution on the Pt/C, $Pt_{90}Sn_{10}$/C and $Pt_{80}Sn_{10}M_{10}$/C (M = Rh, Pd, Ni, Co) electrodes with a scan rate of 1 mV s^{-1}. (For interpretation of the references to colour in this figure legend, the reader is referred to the web version of the article.)

solution with a scan rate of 1 mV s^{-1}. Noticeably, the voltammetric behaviour of $Pt_{80}Sn_{10}Ni_{10}/C$ is similar to that of $Pt_{80}Sn_{10}Co_{10}/C$ since their current gains a pronounced hump in the potential range of 0.1–0.7 V vs. RHE. This hump-shaped current is probably due to the highly oxophilic nature of Co and Ni.

IR spectra of adsorption and oxidation of acetaldehyde on the Pt/C, $Pt_{90}Sn_{10}/C$ and $Pt_{80}Sn_{10}M_{10}/C$ (M = Ni, Co, Rh, Pd) catalysts are presented in Figs. 2 and 3. The CO_2 and calculated CO region are also displayed on expanded scales. According to the spectra, two bands at 1400–1420 cm^{-1} and 1275–1285 $cm^{-1}$are observed, corresponding to the acetate ions [17–19] and acetic acid [18], respectively. On the other hand the presence of linearly bonded CO_L (2040–2050 cm^{-1}) and CO_2 (2345 cm^{-1}) bands in all electrodes is an indicative of the cleavage of C–C bond in acetaldehyde. Moreover, it is interesting to note that $Pt_{80}Sn_{10}Ni_{10}/C$ and $Pt_{80}Sn_{10}Rh_{10}/C$ electrodes shows the formation of bridge bonded CO_B (1822–1848 cm^{-1}) in addition to the linearly bonded CO_L (2040–2050 cm^{-1}), suggesting that acetaldehyde is dissociatively adsorbed at low potentials on these electrodes. On $Pt_{90}Sn_{10}/C$, $Pt_{80}Sn_{10}Ni_{10}/C$, $Pt_{80}Sn_{10}Co_{10}/C$ and $Pt_{80}Sn_{10}Rh_{10}/C$ electrodes, a positive-going band around 1600–1650 cm^{-1} due to the bending mode of liquid water (δ_{HOH}) [20], which is increased with the potential. In the case of $Pt_{80}Sn_{10}Pd_{10}/C$, the negative-going band in the spectral region of 1600–1620 cm^{-1} is attributed to the formation of adsorbed acetyl species [17,21–24], which dissociates to CO_{ad} and CH_x. This band at ca. 1613 cm^{-1} is also observed on Pt/C at very low potential (Fig. 2a). When CO is formed on $Pt_{80}Sn_{10}Pd_{10}/C$ at the potential higher than 0.2 V, the band intensity of acetyl species started to decrease due to blockage of the catalyst active sites, which are necessary for the further dissociation of adsorbed acetyl species, by the accumulation of CO_{ad} and CH_x. When the CO_{ad} is totally oxidized to CO_2 at around 0.6 V, the adsorption of acetyl

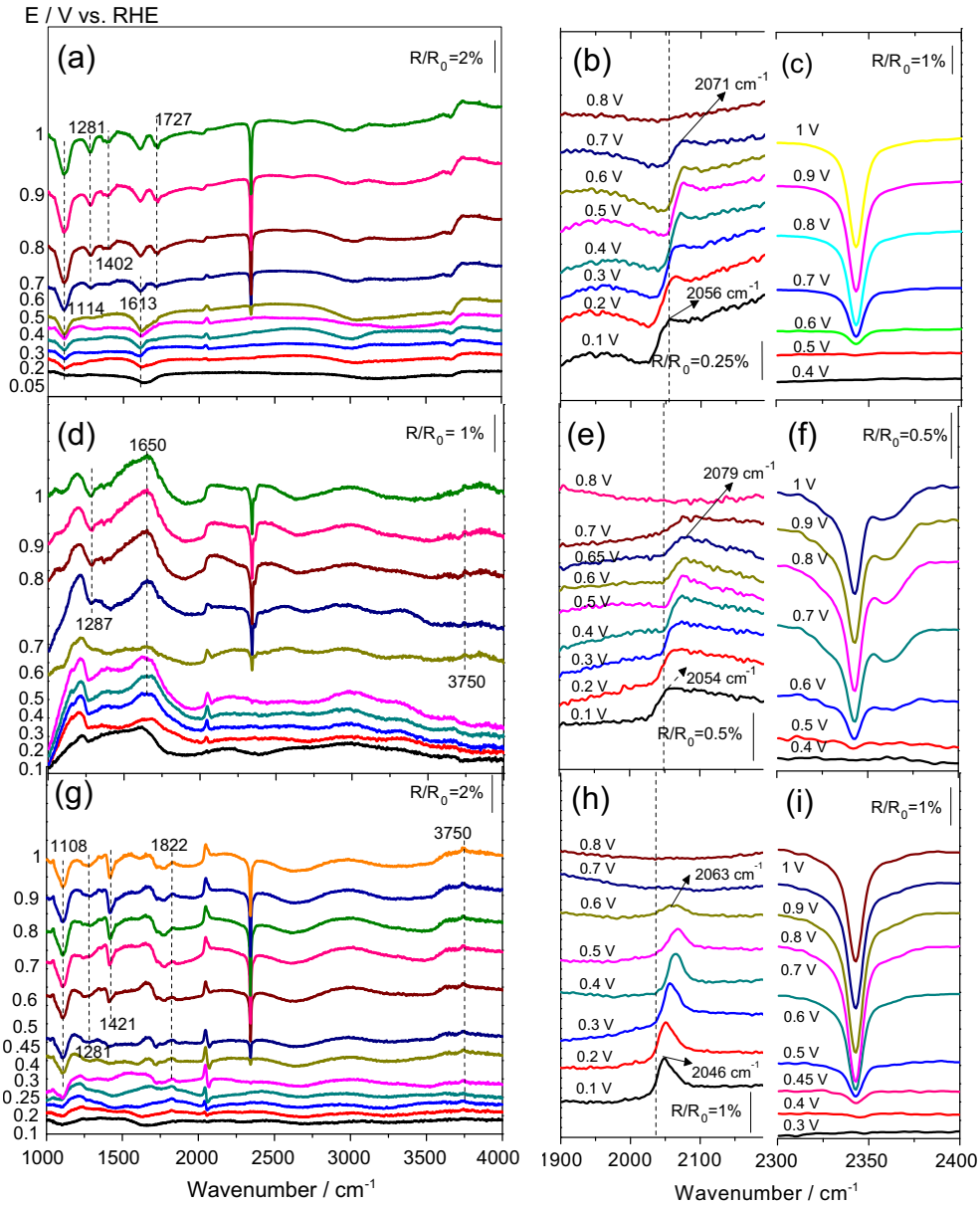

Fig. 2. IR spectra obtained on Pt/C (a, b, c), $Pt_{90}Sn_{10}/C$ (d, e, f) and $Pt_{80}Sn_{10}Ni_{10}/C$ (g, h, i) electrodes in 0.1 M CH_3CHO + 0.1 M $HClO_4$. The reference spectrum was collected at 0.05 V vs. RHE and the sample spectra were taken after applying potential steps towards more positive potentials. The CO region (b, e, h) was calculated with a reference spectrum taken at 0.9 V vs. RHE, i.e., after complete CO oxidation. The CO_2 region (c, f, i) was calculated with a reference spectrum taken at 0.05 V vs. RHE, i.e., before CO oxidation.

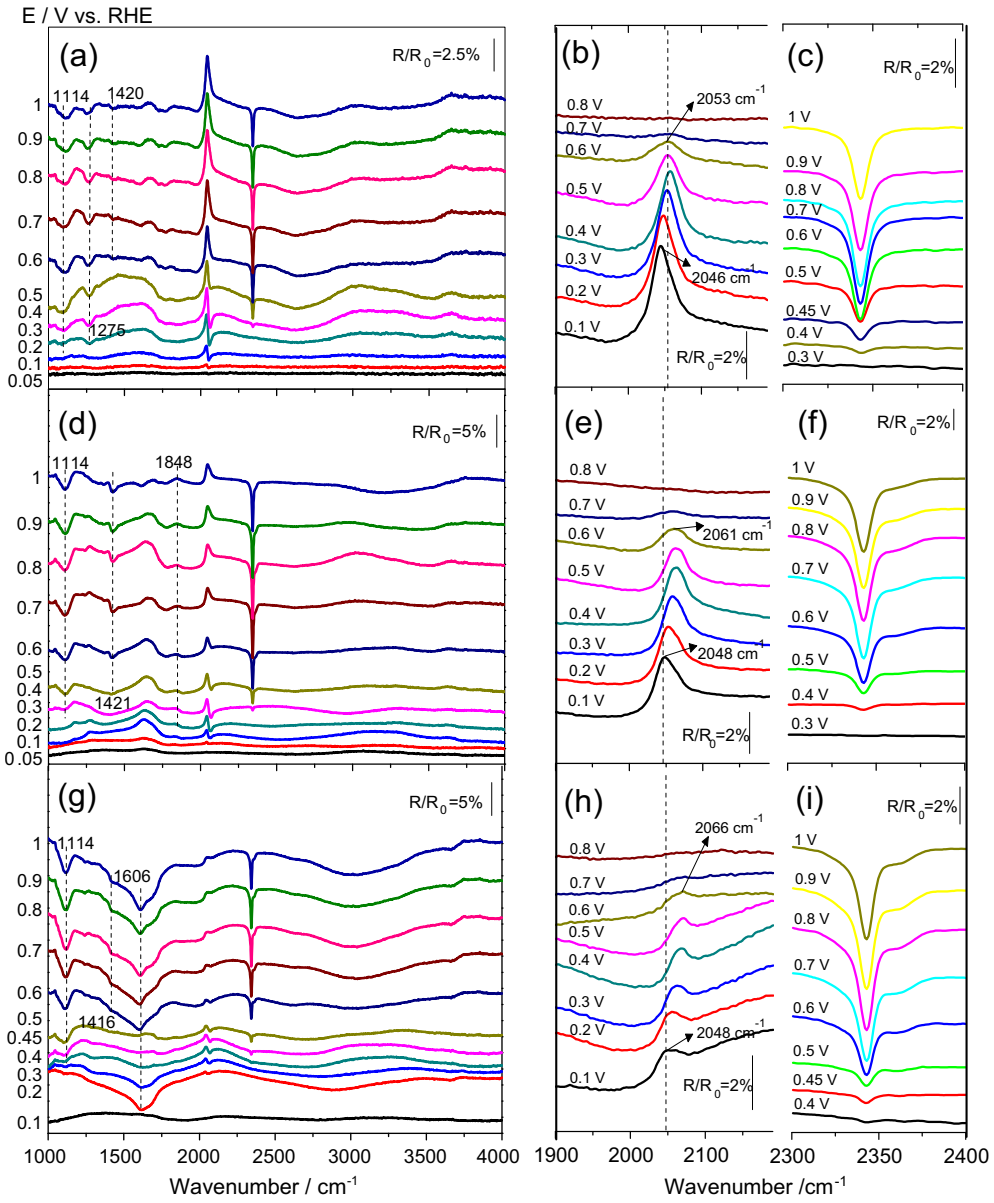

Fig. 3. IR spectra obtained on $Pt_{80}Sn_{10}Co_{10}/C$ (a, b, c), $Pt_{80}Sn_{10}Rh_{10}/C$ (d, e, f) and $Pt_{80}Sn_{10}Pd_{10}/C$ (g, h, i) electrodes in 0.1 M CH_3CHO + 0.1 M $HClO_4$. The spectra were obtained and computed as described in Fig. 2.

species is increased again. Unfortunately, the changes of the interfacial water band at around 1650 cm^{-1} [20] can affect the band intensity of adsorbed acetyl species, thus we cannot evaluate this band properly. With the help of surface oxides on $Pt_{80}Sn_{10}Pd_{10}/C$ at higher than 0.7 V, acetate species is also formed. The formation of acetyl species is obviously favoured on $Pt_{80}Sn_{10}Pd_{10}/C$ during the oxidation of acetaldehyde, which is different from the other PtSn-based trimetallic catalysts. This result is supported by our forthcoming publication that will show the formation of acetic acid at very low potential on $Pt_{80}Sn_{10}Pd_{10}/C$ catalyst based on IR measurements during the electrooxidation of ethanol [25]. The IR results for $Pt_{80}Sn_{10}Rh_{10}/C$ catalyst show the adsorbed both CO_L and CO_B species, which could be explained by the highest level of CO_2 formation. Surprisingly, there is no IR band related to the formation of acetic acid on $Pt_{80}Sn_{10}Rh_{10}/C$; however, acetate species is formed at 0.5 V in parallel to the formation of CO_2. Since the adsorbed CO_{ad} is oxidized at higher than 0.6 V, there should be other intermediates than CO_{ad} to be further oxidized to CO_2. It is reasonable to suggest that adsorbed acetate may be decomposed to carbonate which is further oxidized to CO_2. However, this is an open question since the adsorbed acetate cannot be oxidized further at room temperature and is in reversible equilibrium with acetic acid in the bulk electrolyte. During the electrooxidation of acetaldehyde on $Pt_{80}Sn_{10}Co_{10}/C$ catalyst, the adsorbed CO_{ad} is considerably increased with increasing the potential. On the other hand, the formation of acetic acid is observed at 0.3 V, possibly due to the route involving the OH groups on the surface of $Pt_{80}Sn_{10}Co_{10}/C$.

The band intensity for CO_L and CO_2 are plotted together as a function of applied potential in the Fig. 4. The band frequencies for linearly bonded CO_L versus potential are also shown for all electrodes in the insets of Fig. 4. The relationship between CO_L band frequency (υ) and the electrode potential (E) is termed as the "Stark tuning rate" ($cm^{-1}\ V^{-1}$). This value is found to be 45 $cm^{-1}\ V^{-1}$ at low CO coverage (<0.13 ML) on a polycrystalline Pt electrode in

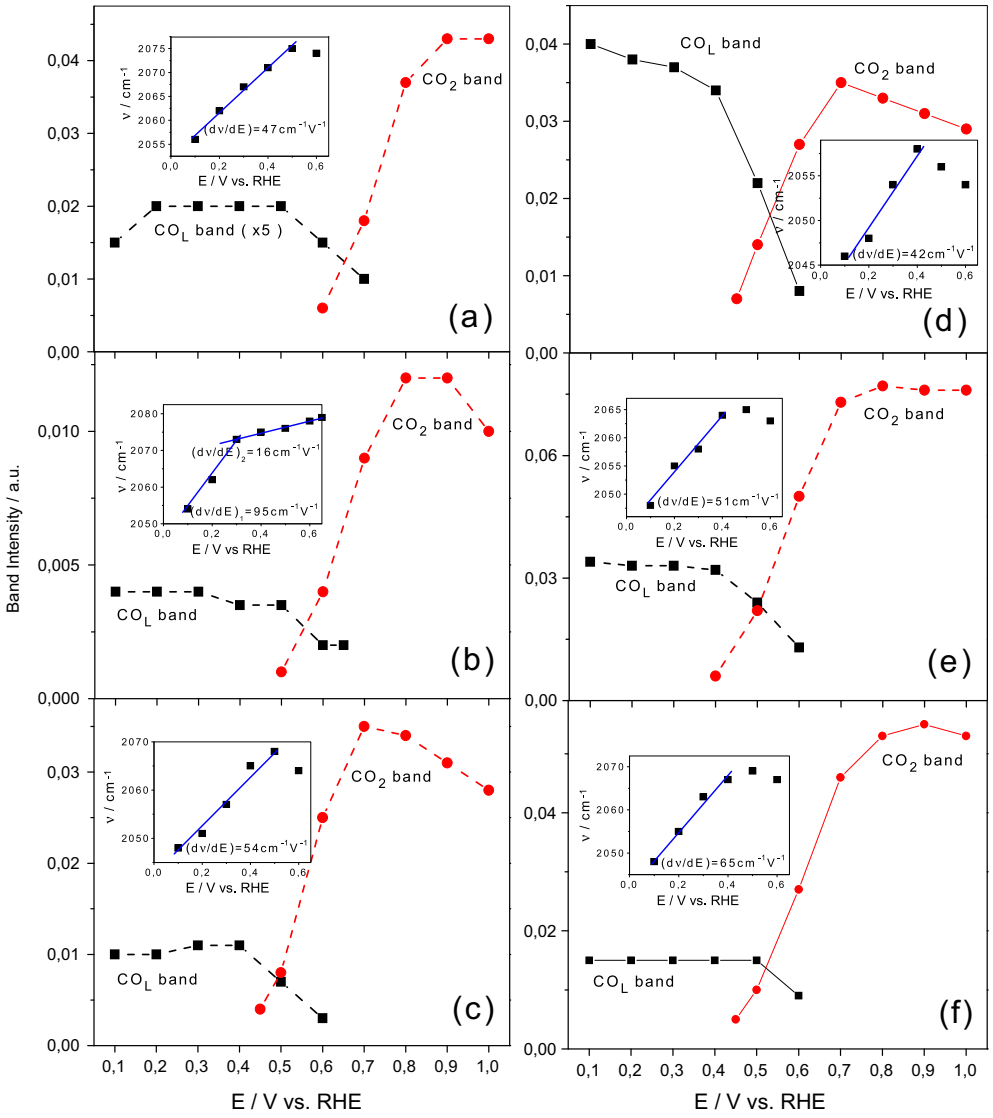

Fig. 4. Potential dependence of the band intensities for CO_2 (2345 cm^{-1}) and CO_L (2040–2050 cm^{-1}) formed during the first anodic polarization of Pt/C (a), $Pt_{90}Sn_{10}$/C (b), $Pt_{80}Sn_{10}Ni_{10}$/C (c), $Pt_{80}Sn_{10}Co_{10}$/C (d), $Pt_{80}Sn_{10}Rh_{10}$/C (e) and $Pt_{80}Sn_{10}Pd_{10}$/C (f) electrodes in 0.1 M CH_3CHO + 0.1 M $HClO_4$, Insets: corresponding the potential dependence of the band centre frequency for linearly bonded CO_L (from the IR spectra in Figs. 2 and 3).

aqueous electrolyte; however, at saturation coverage (~0.65 ML) decreased down to 30 cm^{-1} V^{-1} [26–31]. In our study, the CO_L vibrational Stark tuning rate (ν–E slope) is found to be around 42–65 cm^{-1} V^{-1}, except for $Pt_{90}Sn_{10}$/C electrode. Because the CO_L band frequency for this electrode exhibits two different behaviours for two potential regions (Fig. 4b). Below 0.3 V, a high initial slope value (95 cm^{-1} V^{-1}) and another different behavior above 0.6 V with a slope about 16 cm^{-1} V^{-1}, indicates that the adsorption of CO occurs in the initial stages at a very low coverage. For all electrodes, the CO_L stretching vibrational frequency varies linearly in the potential range of 0.1–0.5 V vs. RHE (Fig. 4). Above ca. 0.4 V vs. RHE, where CO_L starts being oxidized, the CO_L band frequency decreases. This can be interpreted as a red-shift. Noticeably, the CO_L band intensity of $Pt_{80}Sn_{10}Co_{10}$/C electrode is decreased severely at potential higher than 0.45 V vs. RHE with a concomitant increase in the formation of CO_2, suggesting that the CO_2 is formed directly from initially adsorbed CO species. Moreover, the partial oxidation of acetaldehyde to CO is confirmed by an increase in the current for $Pt_{80}Sn_{10}Co_{10}$/C electrode in the potential range of 0.1–0.45 V vs. RHE (Fig. 1). It can be seen from the IR spectra that acetic acid is also formed at higher than 0.4 V (Fig. 3a). The adsorption of acetaldehyde seems to reach the saturation on the active surface sites since there is a no change in the current response up to a potential of about 0.7 V (Fig. 1), where the adsorbed CO is totally consumed on the surface. Therefore, the potential range between 0.4 and 0.7 V, there may be a competition for the formation between acetic acid and CO_2 through surface oxides on the active sites.

The comparison of IR band intensities for CO_L and CO_2 species formed during the adsorption and oxidation of acetaldehyde is tabulated in Fig. 5. At 0.5 V vs. RHE, there is a substantial CO poisoning on the surface of $Pt_{80}Sn_{10}Rh_{10}$/C and $Pt_{80}Sn_{10}Co_{10}$/C electrodes, which could result from the strong interaction between surface metal atoms and acetaldehyde molecules. Apart from Pt/C, the adsorbed CO_L on the surface is totally oxidized to CO_2 at 0.7 V vs. RHE. Both linearly and bridge bonded CO lead to increase the level of CO_2 production for $Pt_{80}Sn_{10}Ni_{10}$/C and $Pt_{80}Sn_{10}Rh_{10}$/C electrodes. The production of CO_2 during oxidation of the acetaldehyde solution on $Pt_{80}Sn_{10}Rh_{10}$/C electrode is higher than those obtained on other electrodes, suggesting that Rh can promote the breaking C–C bond. This hypothesis has also been proposed by several authors in

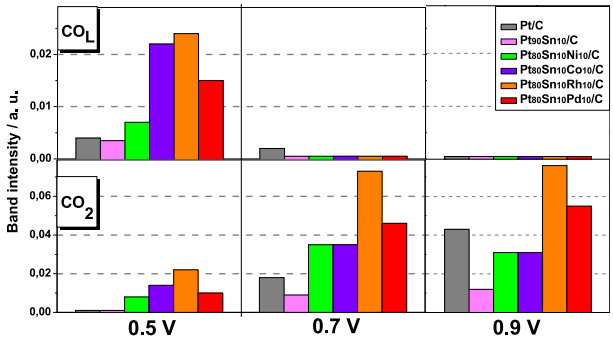

Fig. 5. Comparison of the CO_2 and CO_L band intensities for Pt/C, bimetallic $Pt_{90}Sn_{10}$/C and trimetallic $Pt_{80}Sn_{10}M_{10}$/C (M = Ni, Co, Rh and Pd) electrodes in 0.1 M CH_3CHO + 0.1 M $HClO_4$ at 0.5, 0.7 and 0.9 V vs. RHE (from the IR spectra in Figs. 2 and 3). (For interpretation of the references to colour in this figure legend, the reader is referred to the web version of the article.)

terms of the highest ethanol conversion of Rh over noble metals (Pt, Ru, and Pd) [32–36]. $Pt_{90}Sn_{10}$/C electrode is not very selective for the production of CO_2. Since acetaldehyde adsorbed weakly on the sites of Pt due to the electronic influence of Sn, the most of acetaldehyde then can be desorbed from the electrode surface (Eq. (1)).

$$Pt(CH_3CHO)_{ads} \rightarrow (CH_3CHO)_{sol} + Pt \quad (1)$$

On the other hand, probably a higher amount of SnO_2 favors the interfacial water (1650 cm^{-1}) (Fig. 2d), which hinders the initial adsorption of acetaldehyde and consequently lowers the activity for the cleavage of C–C bond in acetaldehyde. Therefore, the reaction pathway from acetaldehyde to CO_{ads} is less pronounced on $Pt_{90}Sn_{10}$/C electrode (Eqs. (2) and (3)).

$$Pt(CH_3CHO)_{ads} \rightarrow Pt(CH_3CO)_{ads} + H^+ + e^- \quad (2)$$

$$Pt(CH_3CHO)_{ads} \rightarrow Pt(CO)_{ads} + Pt(CH_3)_{ads} \quad (3)$$

The instant decrease in the CO_L band intensity at 0.4 V vs. RHE when just the beginning to form of CO_2, clearly confirms that the oxygenated species supplied by Sn surface atoms lead the oxidation of the adsorbed CO on the Pt to CO_2 according to the Eqs. (4) and (5).

$$H_2O + Sn \rightarrow Sn(OH)_{ads} + H^+ + e^- \quad (4)$$

$$Pt(CO)_{ads} + Sn(OH)_{ads} \rightarrow Pt + Sn + CO_2 + H^+ + e^- \quad (5)$$

Because of the low level production of CO_2 on the $Pt_{90}Sn_{10}$/C electrode, the oxidation of acetaldehyde to acetic acid is more likely to occur (Eq. (6)).

$$Pt(CH_3CHO)_{ads} + Sn(OH)_{ads} \rightarrow Pt + Sn + CH_3COOH + H^+ + e^- \quad (6)$$

According to the obtained in-situ IR results, the reaction mechanism of the adsorption and electrooxidation of acetaldehyde on Pt/C, $Pt_{90}Sn_{10}$/C, $Pt_{80}Sn_{10}M_{10}$/C (M = Ni, Co, Rh, Pd) electrodes can be schematically summarized in Fig. 6. It has previously been reported that CH_3CHO can adsorb on surface through the oxygen lone pair electrons (CH_3CHO^*) or in a configuration where both the carbonyl carbon and oxygen atoms ($CH_3C^*HO^*$) interact with the surface [23]. The first configuration produces a weak surface-aldehyde bonding, as a result, molecularly desorption occurs. However, the second type of configuration results in stronger surface-aldehyde bonding which leads to the competition between desorption and decomposition reactions. In this sense, we would expect that acetaldehyde adsorbs weakly on the surface of $Pt_{90}Sn_{10}$/C via oxygen lone pair electrons,

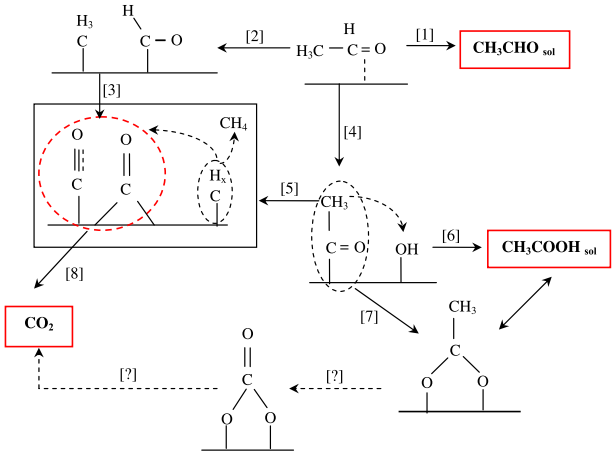

Fig. 6. Scheme of reaction mechanism proposed for the adsorption and oxidation of acetaldehyde on Pt/C, bimetallic $Pt_{90}Sn_{10}$/C, and trimetallic $Pt_{80}Sn_{10}M_{10}$/C (M = Ni, Co, Rh, Pd) electrodes.

and consequently tends to desorb from the surface to the solution by reaction 1. In the case of a strong adsorption of acetaldehyde on the surface via both the carbonyl carbon and oxygen atoms, acetyl (CH_3CO) species are formed which can react with the OH species to give rise to the CH_3COOH (reactions 4 and 6). In the presence of surface oxygen groups on the carbon, CH_3CO can be converted to acetate (CH_3COO) species (reaction 7), which are in equilibrium with the CH_3COOH solution. On the other hand, CH_3CO can be decomposed to CH_x and CO species by reaction 5. At low potential, the adsorbed CH_3 and CHO species are formed by the dissociative adsorption of acetaldehyde (reaction 2), which can also convert to CO species (reaction 3) and finally, oxidize to CO_2 by reaction 8.

4. Conclusions

The adsorption and oxidation of acetaldehyde on the Pt/C, $Pt_{90}Sn_{10}$/C and $Pt_{80}Sn_{10}M_{10}$/C (M = Ni, Co, Rh, Pd) electrodes was investigated by in situ FTIR spectroscopy measurements. As a function of the applied potentials, the intermediates and products were identified. IR results for the oxidation of acetaldehyde on carbon supported PtSn and PtSn-based trimetallic catalysts show the formation of adsorbed linearly bonded CO_L, bridge-bonded CO_B, acetyl species, acetate, and acetic acid. However, a slight discrepancy of the product distribution of the oxidation of acetaldehyde depends on the presence of a third metal in PtSn-based catalyst. The IR results suggest that the addition of third metal to PtSn/C catalyst promotes the cleavage of the C–C bond of acetaldehyde. $Pt_{80}Sn_{10}Rh_{10}$/C showed the highest efficiency in the production of CO_2 in parallel with the high level of CO_{ads} poisoning on its surfaces. On the other hand, the reaction pathway of CO_2 production seems to originate from the formation of CH_3CO species, which is favoured on $Pt_{80}Sn_{10}Pd_{10}$/C catalyst.

Acknowledgement

This work was carried out within the framework of a bilateral cooperation programme between Istanbul Technical University (Turkey) and Université de Poitiers (France). S. B. thanks Bourse du Gouvernement Français (Contract # 20064739) for support.

References

[1] B. Rasch, T. Iwasita, Electrochim. Acta 35 (1990) 989–993.
[2] J.L. Rodriguez, E. Pastor, X.H. Xia, T. Iwasita, Langmuir 16 (2000) 5479–5486.

[3] J. Silva-Chong, E. Méndez, J.L. Rodriguez, M.C. Arévalo, E. Pastor, Electrochim. Acta 47 (2002) 1441–1449.
[4] K.B. Kokoh, F. Hahn, E.M. Belgsir, C. Lamy, A.R. De Andrade, P. Olivi, A.J. Motheo, G. Tremiliosi-Filho, Electrochim. Acta 49 (2004) 2077–2083.
[5] J. Willsau, J. Heitbaum, J. Electroanal. Chem. 194 (1985) 27–35.
[6] G.A. Camara, T. Iwasita, J. Electroanal. Chem. 578 (2005) 315–321.
[7] S.C. Chang, L.W.H. Leung, M.J. Weaver, J. Phys. Chem. 94 (1990) 6013–6021.
[8] H. Wang, Z. Jusys, R.J. Behm, J. Phys. Chem. B 108 (2004) 19413–19424.
[9] J.F. Gomes, B. Busson, A. Tadjeddine, J. Phys. Chem. B 110 (2006) 5508–5514.
[10] X.H. Xia, H.D. Liess, T. Iwasita, J. Electroanal. Chem. 437 (1997) 233–240.
[11] H. Bönnemann, W. Brijoux, Catalytic active metal powders and colloids, in: VCH (Ed.), Active Metals: Preparation, Characterization, Applications, Germany, Weinheim, 1995, pp. 339–378.
[12] S. Beyhan, J.-M. Léger, F. Kadırgan, Appl. Catal. B Environ. 130 (2013) 305–313.
[13] S. Beyhan, C. Coutanceau, J.-M. Léger, T.W. Napporn, F. Kadırgan, Int. J. Hydrogen Energy 38 (2013) 6830–6841.
[14] D. Lambert, Electrochim. Acta 41 (1996) 623–630.
[15] F.C. Nart, T. Iwasita, Electrochim. Acta 41 (1996) 631–636.
[16] F. Maillard, F. Gloaguen, F. Hahn, J.-M. Léger, Fuel Cells 3 (2002) 143–152.
[17] A. Rodes, E. Pastor, T. Iwasita, J. Electroanal. Chem. 376 (1994) 109–118.
[18] D.S. Corrigan, E.K. Krauskopf, L.M. Rice, A. Wieckowski, M.J. Weaver, J. Phys. Chem. 92 (1988) 1596–1601.
[19] K. Ito, H.J. Bernstein, Can. J. Chem. 34 (1956) 170–178.
[20] A. Miki, S. Ye, M. Osawa, Chem. Commun. (2002) 1500–1501.
[21] M.H. Shao, R.R. Adzic, Electrochim. Acta 50 (2005) 2415–2422.
[22] M. Heinen, Z. Jusys, R.J. Behm, J. Phys. Chem. C 114 (2010) 9850–9864.
[23] J.L. Davis, M.A. Barteau, J. Am. Chem. Soc. 111 (1989) 1782–1792.
[24] R. Shekhar, M.A. Barteau, R.V. Plank, J.M. Vohs, J. Phys. Chem. B 101 (1997) 7939–7951.
[25] S.Beyhan, J.-M.Léger, F.Kadırgan, Appl. Catal. B Environ., submitted for publication.
[26] S.-C. Chang, M.J. Weaver, Surf. Sci. 238 (1990) 142.
[27] S.-C. Chang, M.J. Weaver, J. Phys. Chem. 92 (1990) 4582.
[28] J.W. Russell, M. Severson, K. Scanlon, J. Overend, A. Bewick, J. Phys. Chem. 87 (1983) 293–297.
[29] K. Kunimatsu, W.G. Golden, H. Seki, M.R. Philpott, Langmuir 1 (1985) 245–250.
[30] K. Kunimatsu, K. Shimazu, H. Kita, J. Electroanal. Chem. 256 (1988) 371–385.
[31] J. Lu, A. Bewick, J. Electroanal. Chem. 270 (1989) 225–235.
[32] J.P. Breen, R. Burch, H.M. Coleman, Appl. Catal. B 39 (2002) 65–74.
[33] F. Frusteri, S. Freni, L. Spadaro, V. Chiodo, G. Bonura, S. Donato, Catal. Commun. 5 (2004) 611–615.
[34] D.K. Liguras, D.I. Kondarides, X.E. Verykios, Appl. Catal. B 43 (2003) 345–354.
[35] J.R. Salge, G.A. Deluga, L.D. Schmidt, J. Catal. 235 (2005) 69–78.
[36] P.Y. Sheng, H. Idriss, J. Vac. Sci. Tech. A 22 (2004) 1652–1658.